

Features of shear transformation texture in seamless pipes

Cite as: AIP Conference Proceedings **2053**, 040051 (2018); <https://doi.org/10.1063/1.5084489>
Published Online: 19 December 2018

M. L. Lobanov, I. Yu. Pyshmintsev, A. N. Maltseva, D. P. Uskov, S. V. Danilov, E. A. Makarova, and V. I. Pastukhov



View Online



Export Citation

ARTICLES YOU MAY BE INTERESTED IN

[Evolution of microstructure in stainless martensitic steel for seamless tubing](#)

AIP Conference Proceedings **1915**, 040048 (2017); <https://doi.org/10.1063/1.5017396>

[Specific effects of microalloying elements on the development of the strength properties of low-alloyed chromium-molybdenum pipe steels](#)

AIP Conference Proceedings **2053**, 030056 (2018); <https://doi.org/10.1063/1.5084417>

AIP | Conference Proceedings

**Get 30% off all
print proceedings!**

Enter Promotion Code **PDF30** at checkout



Features of Shear Transformation Texture in Seamless Pipes

M. L. Lobanov^{1, a)}, I. Yu. Pyshmintsev^{2, b)}, A. N. Maltseva^{2, c)}, D. P. Uskov^{3, d)},
S. V. Danilov^{1, e)}, E. A. Makarova^{1, f)}, and V. I. Pastukhov^{1, 4, g)}

¹*B. N. Yeltsin Ural Federal University, 19 Mira St., Ekaterinburg, 620002, Russia*

²*ROSNITI JSC, 30 Novorossiyskaya St., Chelyabinsk, 454139, Russia*

³*Volzhsky Pipe Plant, 6 Avtodoroga 7 St., Volzhsky, 404119, Russia*

⁴*Institute of Nuclear Materials JSC, P. Box 29, Zarechny, 624250, Russia.*

^{a)}Corresponding author: m.l.lobanov@urfu.ru

^{b)}PyshmintsevIU@sinara-group.com

^{c)}maltsevaan@rosniti.ru

^{d)}UskovDP@vtz.ru

^{e)}s.v.danilov@bk.ru

^{f)}makarova-zhenechka94@mail.ru

^{g)}vladimir.pastuhov@urfu.ru

Abstract. Microstructure and texture in seamless 0.08C–Cr–Mo–V, 0.25C–Cr–Mo–V–Nb, 0.08–13Cr–3Ni–Mo–V–Nb, and 18Cr–9Ni steel pipes are studied in the as-rolled and heat-treated states using orientation EBSD microscopy. It has been found that all types of microstructure (ferrite, martensite, and bainite) in products, both after hot rolling and after heat treatment, have well-defined axial crystallographic texture, where the <111> direction is predominately perpendicular to the pipe surface. It is demonstrated that texture formation in heat-treated states is inherited due to the following factors important for the rules of orientation selection during the $\gamma \rightarrow \alpha$ phase transformation: 1) occurrence of stable orientation of austenite grains resulted from straining; 2) special misorientation (boundaries) of austenite grains where transformation starts; 3) orientation relationships known for phase transformation; 4) thermal stresses in a product, formed during cooling. The latter can be considered as factor determining special texture in seamless steel pipes.

INTRODUCTION

The manufacture of structural and functional materials and corresponding products is, as a rule, accompanied by directional straining and thermal cycles. This leads to the formation of a crystallographic microstructure. The occurrence of texture results in a set of orientation-dependent physical and mechanical properties, which should be taken into account in the development of new and improvement of existing technologies [1, 2].

In some cases, the integral texture of a product plays a less important role than one of its weak components. For example, as it was demonstrated in [3–5], a rotated cube component with the (001) plane parallel to the rolling plane plays a significant role in the fracture of steel plates for welded pipes. The existence of coarse elongated grains with this orientation is critical for easy crack nucleation and propagation in such areas.

The aim of this study is to reveal the most general features of crystallographic texture formation in seamless steel pipes during production and use.

RESEARCH METHODS

Typical 0.08C–Cr–Mo–V, 0.25C–Cr–Mo–V–Nb, 0.08–13Cr–3Ni–Mo–V–Nb, and 18Cr–9Ni steels were used as materials for the study. Specimens were taken along the production route after hot deformation in the austenite range after quenching with tempering. The 0.08C–18Cr–9Ni stainless steel was used after long-time operation at elevated

temperatures. Operation at high temperatures resulted in deep decarburization of the steel, and that was the reason for the shift of shear transformation temperature above the ambient. Details are given in Table 1.

TABLE 1. Grades, sizes, microstructure types and heat treatment of the studied pipes

Grade	Ø/wt, mm	Microstructure in hot-rolled state	Heat treatment	Microstructure in heat-treated state
0.08C–Cr–Mo–V	273/8	Ferrite and pearlite	Quenched 920 °C, tempered at 650 °C	Tempered martensite and bainite
0.25C–Cr–Mo–V–Nb	245/14	Ferrite and pearlite	Quenched 900 °C, tempered at 600 °C	Tempered martensite
0.08–13Cr–3Ni–Mo–V–Nb	127/6	Martensite and δ -ferrite	Quenched 950 °C, tempered at 620 °C	Tempered martensite
18Cr–9Ni	950/20	Austenite	Years of operation at above 400 °C	Austenite

Polished sections for a metallographic study were prepared in the RD–ND plane (where RD is the rolling direction and ND is the normal direction), which is normal to the hoop direction in the pipe. Electron microscopy was carried out using a Zeiss Crossbeam Auriga microscope at an acceleration voltage of 20 kV. An EBSD HKL Inca unit with an Oxford Instruments analysis system was used for grain orientation determination and texture analysis. The scanning step was varied between 0.1 and 2 μm depending on the task of misorientation measurement for each grain or general texture for the full cross-section area. The error in the orientation measurement was no higher than $\pm 1^\circ$ ($\pm 0.6^\circ$ on the average). The low-angle boundaries between local areas were defined for 2–15° misorientations, and they are shown in 1 pixel lines. The high-angle boundaries with a misorientation of above 15° were set as coarse 2 pixel lines. All possible orientations of the crystals were determined by analyzing the orientation functions. The main texture components were determined from the $\{100\}$, $\{110\}$, and $\{111\}$ direct pole figures.

RESULTS AND DISCUSSION

Depending on the chemical composition and the cooling rate, ferrite and pearlite were revealed in the microstructure of the 0.08C–Cr–Mo–V and 0.25C–Cr–Mo–V–Nb steels after hot rolling (Fig. 1a). Martensite and some amount of δ -ferrite were found in the 0.08–13Cr–3Ni–Mo–V–Nb steel in the hot-deformed state (Fig. 1b), and austenite was found in 18Cr–9Ni (Fig. 2d). The measurements of texture in the hot-deformed state have demonstrated dissolved but clearly visible texture in both ferrite and martensite. This texture contains mainly two symmetrical components of the $\{112\}\langle 110 \rangle$ type (Fig. 1c, d). The austenite texture contains several components: two from the $\{112\}\langle 111 \rangle$ combination and two from $\{110\}\langle 111 \rangle$. Weaker components $\{110\}\langle 001 \rangle$ and $\{100\}\langle 001 \rangle$ are also seen, which are stable deformation orientations, typical of fcc materials according to [6, 7].

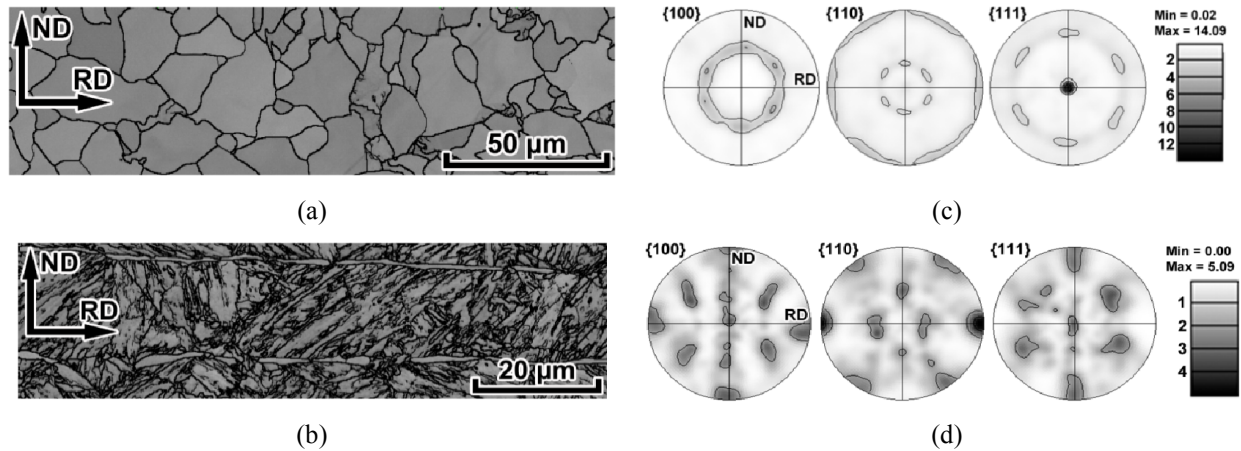


FIGURE 1. Orientation maps with intercrystalline boundaries, plotted by the EBSD method (a, b) and direct pole figures (c, d) for hot-deformed tubulars: a, c – 0.08C–Cr–Mo–V; b, d – 0.08–13Cr–3Ni–Mo–V–Nb

Shear transformation type microstructures were found in all pipes after heat treatment or after operation: bainite and martensite for the 0.08C–Cr–Mo–V steel (Fig. 2a), martensite for the 0.25C–Cr–Mo–V–Nb and 0.08–13Cr–3Ni–Mo–V–Nb steels (Fig. 2b, c). Partial transformation of austenite to bainite was found in the 18Cr–9Ni steel (Fig. 2d). Dissolved texture of $\alpha(\alpha')$ phases was found in all the transformed microstructures, where the main $\{112\}<110>$ components and less pronounced $\{111\}<112>$ and $\{hh1\}<110>$ ones can be easily identified (Fig. 2e–h).

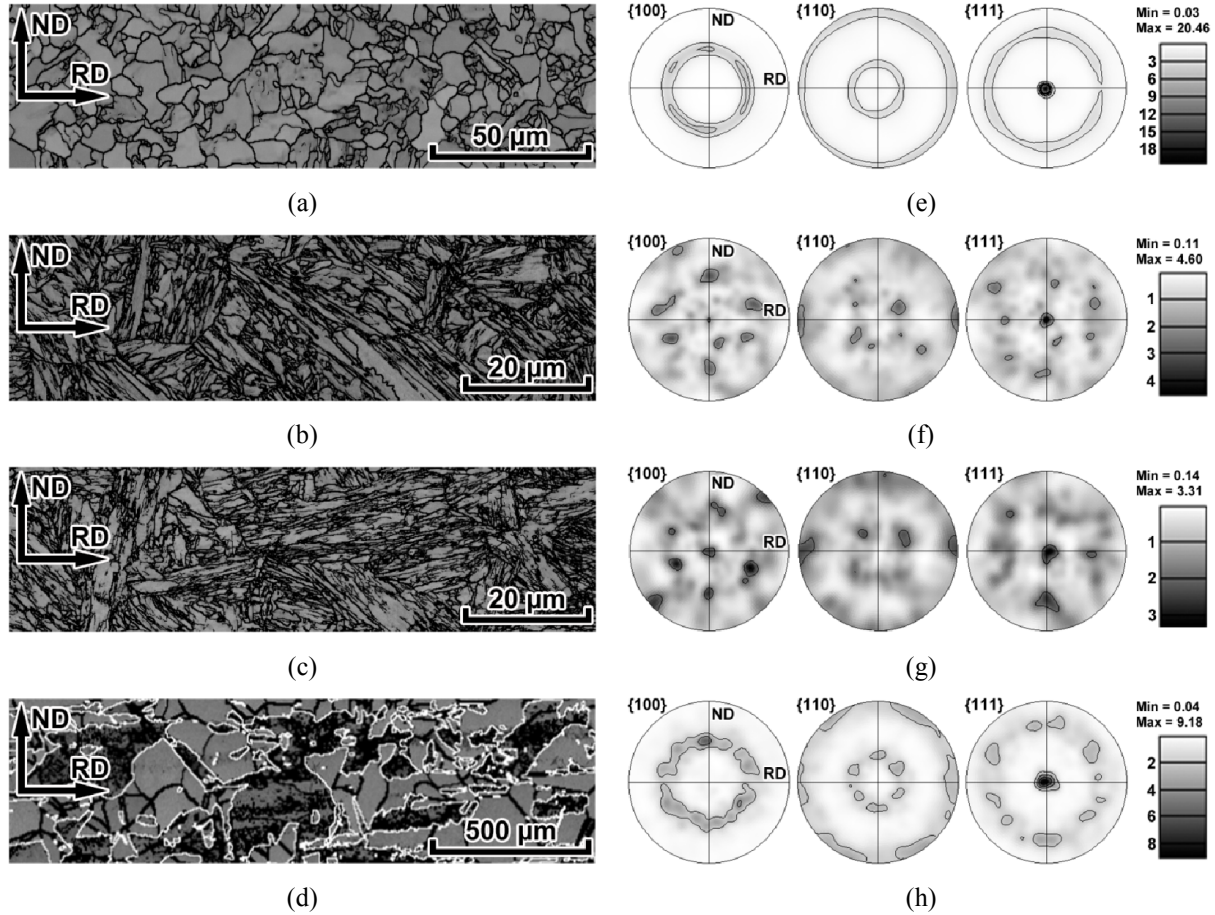


FIGURE 2. Orientation maps with intercrystalline and interphase boundaries, plotted by the EBSD method (a, b, c, d) and direct pole figures (e, f, g, h) for heat-treated tubulars: a, e – 0.08C–Cr–Mo–V; b, f – 0.08–13Cr–3Ni–Mo–V–Nb; c, g – 0.25C–Cr–Mo–V–Nb; d, h – 18Cr–9Ni

The crystallographic analysis of the texture components in the $\alpha(\alpha')$ phases by the method described in [8] has shown for all the cases that the orientations found can be formed from the main orientations of deformed austenite in correspondence with the relationships that are intermediate between the Kurdjumov-Sachs and Nishiyama-Wasserman relationships [6]. The total number of variants is smaller in fact than can be generated theoretically [9, 10].

It is important to note that the main orientations of the $\alpha(\alpha')$ phases after hot deformation and heat treatment are similar. This implies special features leading to inherited textures [11] when the main texture components of deformed austenite are transformed to a limited number of $\alpha(\alpha')$ phase orientations after cooling. During subsequent heating, these orientations will be transformed into the texture of hot-deformed austenite. Quenching of reconstructed austenite will result in the reformation of original orientations in the $\alpha(\alpha')$ phases. According to [11], the factors responsible for such texture reformation can be special CSL-boundaries $\Sigma 3$ and $\Sigma 11$ between deformed austenite grains.

It is remarkable that, in our case, the texture of the $\alpha(\alpha')$ phase can be defined as axial with the $\langle 111 \rangle$ direction parallel to pipe diameter (direct pole figure $\{111\}$, Figs. 1 and 2). Furthermore, for case of the $\alpha \rightarrow \gamma \rightarrow \alpha'$ phase recrystallization in the 0.08C–Cr–Mo–V steel, the texture $\langle 111 \rangle$ of shear phase transformation is even stronger than the texture of ferrite in the hot rolled state. This allows us to suppose that at least one more factor is responsible for texture formation in tubular products resulting from the $\gamma \rightarrow \alpha$ transformation. This factor is thermal stresses (predominately radial) appearing during cooling, with special stress distribution caused by shape symmetry. One of the factors limiting the number of orientations in the product can be slip only in the $\{111\}$ γ planes in austenite. Restrictions in the slip system will lead to higher dislocation density and, correspondingly, to higher values of elastic stress field. The further $\gamma \rightarrow \alpha(\alpha')$ transformation will proceed in accordance with upper orientation relationships for these planes. The latter leads to a limited number of orientations in the $\alpha(\alpha')$ phases within prior austenite grains.

CONCLUSION

It has been demonstrated that texture formation in seamless pipes and textural heredity revealed for heat treatment are caused by the following conditions of defined orientation selection in the $\alpha(\alpha')$ phase at the $\gamma \rightarrow \alpha(\alpha')$ transformation: 1) occurrence of stable orientations of prior austenite grains; 2) special misorientations of CSL boundaries between austenite grains where transformation starts; 3) orientation relationships implemented in the transformation; 4) thermal stresses (mainly radial) induced in the product by cooling.

ACKNOWLEDGMENTS

The work was done using the equipment of the laboratory of Structural Methods of Analysis and Properties of Materials and Nanomaterials of the Collective Use Center affiliated to Ural Federal University. The study of the 18Cr–9Ni steel was supported by of the RFBR, research project No. 18-33-00135-mol_a. The study was supported by the program of increasing the competitiveness of the leading Russian universities, RF Government Resolution No. 211, contract No. 02.A03.21.0006.

REFERENCES

1. A. V. Druker, C. Sobrero, V. Fuster, J. Malarria, and R. Bolmaro, [Advanced Engineering Materials](#) **20**, 1700062 (2018).
2. M. A. Zorina, M. S. Karabanalov, S. I. Stepanov, S. L. Demakov, Yu. N. Loginov, and M. L. Lobanov, [Metall and Mat Trans A](#) **49**, 427–433 (2018).
3. I. Pyshmintsev, A. Gervasyev, R. Kh. Petrov, V. C. Olalla, and L. Kestens, [Materials Science Forum](#) **702–703**, 770–773 (2012).
4. M. A. Mohtadi-Bonab, M. Eskandari, and J. A. Szpunar, [Materials Science and Engineering A](#) **620**, 97–106 (2014).
5. I. Yu. Pyshmintsev, A. O. Struin, A. M. Gervasyev, M. L. Lobanov, G. M. Rusakov, S. V. Danilov, and A. B. Arabey, [Metallurgist](#), **60**, 405–412 (2016).
6. M. Hölscher, D. Raabe, and K. Lücke, [Acta Metall. Mater.](#) **42**, 879–886 (1994).
7. G. M. Rusakov, A. G. Illarionov, Yu. N. Loginov, M. L. Lobanov, and A. A. Redikultsev, [Metal Science and Heat Treatment](#) **56**, 650–655 (2015).
8. M. L. Lobanov, G. M. Rusakov, A. A. Redikultsev, S. V. Belikov, M. S. Karabanalov, E. R. Struina, and A. M. Gervasyev, [Physics of Metals and Metallography](#) **117**, 254–259 (2016).
9. K. Koumatsos and A. Muehleman, [Acta Cryst.](#) **73**, 115–123 (2017).
10. T. Karthikeyan, M. K. Dash, S. Saroja, and M. Vijayalakshmi, [Micron](#) **68**, 77–90 (2015).
11. M. L. Lobanov, M. D. Borodina, S. V. Danilov, I. Yu. Pyshmintsev, and A. O. Struin, [Steel in Translation](#) **47**, 710–716 (2017).